Spectral Characteristics of Coupled Plasmonic Modes in Aggregates of Plasma Columns

Nadiia Stognii, Nataliya Sakhnenko
Department of Higher Mathematics
Kharkiv National University of Radio Electronics
Kharkiv, Ukraine
e-mail: nstognii@gmail.com

***Abstract*— Theoretical study of the eigenfrequencies of coupled plasmons in cylindrical plasma columns is presented. Plasmonic modes of linear chain of coupled plasma cylinders and cluster of square configuration is investigated. Mechanism of the plasmonic mode coupling that can be considered as bonding and antibonding combinations of isolated cylinder plasmons is studied. Accurate analysis of the spectrum of different plasmon resonances and their quality factors is presented.**

Keywords- plasma; surface plasmons; plasmon resonances; eigenfrequency; linear chain; cluster.

I. INTRODUCTION

Surface plasmons are the subject of considerable interest in recent years due to the possibility of strong field enhancement [1 - 2]. Using resonators composed of negative permittivity materials such as plasma can form the basis of effective small-size antenna elements [3]. The main advantage of a plasma antenna over the conventional antennas is due to possibility to control antenna parameters by tuning plasma properties. Various elements such as plasmonic waveguides [4], subwavelength resonators [5] and optical nanoantennas [6] have been studied recently. Plasmonic structures of different shapes (nanowires, nanorods, nanospheres, nanoshells) are provided by various fabrication techniques. The possibility of using plasmonic structures in nanolasers [7] and biosensors [8] is discussed. For these applications an accurate frequency domain modeling that provides a valuable insight into fundamental processes is of great importance.

II. MATHEMATICAL BACKGROUND

In this paper we solve the eigenvalue problem for aggregates of coupled cylindrical plasma columns: a linear chain of coupled plasma cylinders (Fig. 1) and a cluster of square configuration (Fig. 2). Radius of each column is a, separation distance between them is d and plasma is described by the permittivity ε_p that is given by the Drude model

$$\varepsilon_p = 1 - \omega_p^2 \cdot (\omega(\omega + i\gamma))^{-1}, \qquad (1)$$

here ω_p represents the plasma frequency, γ is the material absorption. Sub-wavelength resonances are possible when $\varepsilon(\omega) < 0$ (or equivalently $\omega_p > \omega$), they are called plasmon resonances or surface plasmons. The ambient medium is free space. H-polarized fields are considered. We present the z-component of the internal field as

$$H^{in}(\rho_n, \varphi_n) = \sum_{s=-\infty}^{+\infty} A_s^{(n)} J_s(k_p \rho_n) e^{is\varphi_n}, \qquad (2)$$

and the external field as

$$H^{out}(\rho_n, \varphi_n) = \sum_{n=1}^{N} \sum_{s=-\infty}^{+\infty} \overline{A}_s^{(n)} H_s^{(2)}(k\rho_n) e^{is\varphi_n}, \qquad (3)$$

here (ρ_n, φ_n) are set of N polar systems of coordinates, associated with each cylindrical columns ($n = 1...N$), $z-$ axis is parallel to the cylinders, $k = \omega \cdot c^{-1}$, $k_p = n_p \omega c^{-1}$, c is light velocity in a vacuum, $n_p = \sqrt{\varepsilon_p(\omega)}$, $\varepsilon_p(\omega)$ is defined by formula (1), time dependence is $e^{i\omega t}$.

Unknown coefficients A_s and $\overline{A}_s$ are found from the boundary conditions, requiring the continuity of the tangential components of the total electric and magnetic fields at each cylindrical column's surface. Using the addition theorem for the Bessel functions we arrive to an infinite system of algebraic equations that can be truncated in order to provide a controlled numerical precision. We have to mention that all eigenfrequencies are complex $\omega = \omega' + i\omega''$, where $\omega'' > 0$ represents damping and ω' is associated with the eigen oscillation frequencies. Quality (Q) factor of plasmons can be evaluated through the formula $Q = \omega'/2\omega''$.

III. RESULTS

We start with eigenvalue problem of an isolated plasma cylinder. Figure 3 illustrates the value of the real part of plasmon eigenfrequency versus normalized frequency (ka) for different values of $w_p = \omega_p a c^{-1}$ that we will call further a normalized plasma frequency. We have to stress that there is no solution for the case $s = 0$ (s is a numbers of angular field variations). It is seen that plasmon resonances for different values of s are closely spaced. Field portraits of the plasmons are shown in the inset in Fig. 3 (upper left-hand corner for $s = 1$, lower right-hand corner for $s = 2$, $w_p = 0.5$). Plasmons

with $s=1$ can be considered as dipole plasmon modes, $s=2, 3,...$ as multipole plasmon modes.

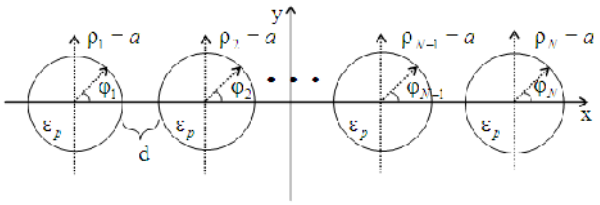

Fig. 1. Schematic diagram of the structure under consideration: a linear chain of coupled plasma cylinders.

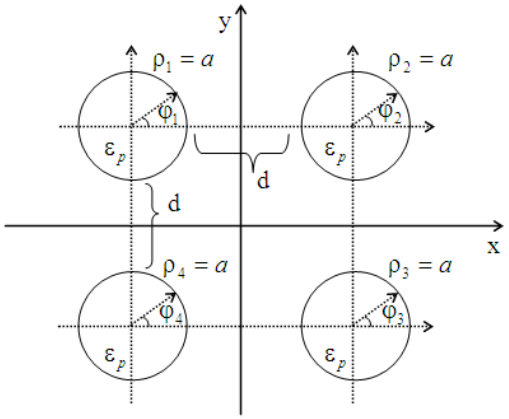

Fig. 2. Schematic diagram of the structure: a cluster of square configuration.

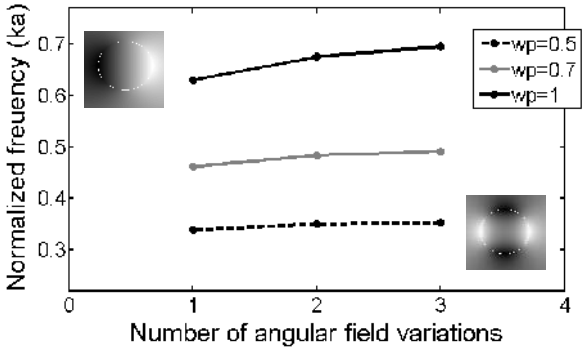

Figure 3. Dependence of the eigenfrequency on the number of angular field variations for different values of the normalized plasma frequency w_p for isolated cylinder.

Figure 4 shows scattering cross section versus normalized frequency (ka) for different values of w_p. For the value of w_p =0.5 we can see only one peak for $\gamma = 10^{-3} w_p$ associated with excited dipole plasmon, additional sharp peak is observable in the spectrum for smaller value of losses $\gamma = 10^{-2} w_p$ associated with quadrupole plasmon. With growing of w_p that can be viewed as increasing of column radius we can see the appearance of quadrupole mode in the spectrum.

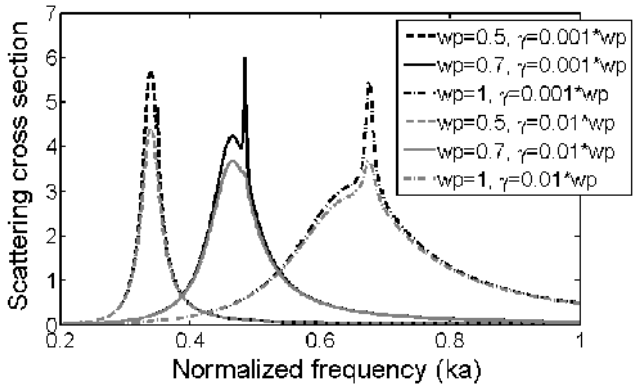

Figure 4. Scattering cross section of isolated plasma column versus normalized frequency (ka) for different values of the normalized plasma frequency.

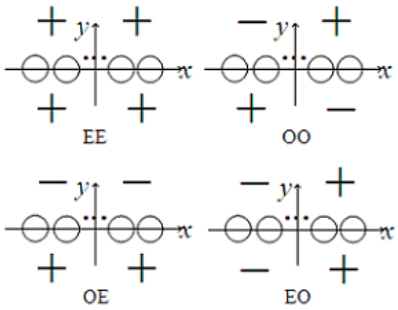

Fig. 5. Four classes of symmetry of the excited plasmons: (a) EE (x - even, y - even), (b) OO (x - odd, y - odd), (c) OE (x - odd, y - even), (d) EO (x - even, y - odd).

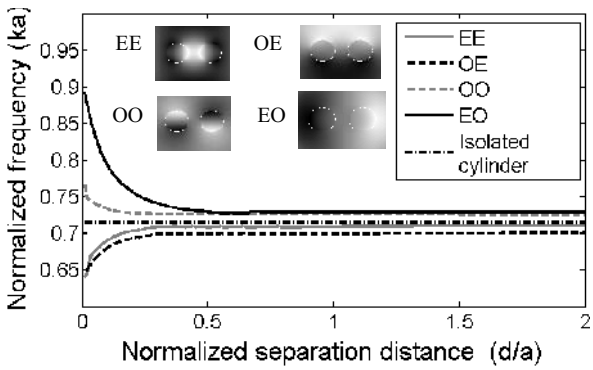

Figure 6. The normalized frequency versus the normalized separation distance between the two coupled plasma cylinders for EE, OE, EO, OO plasmons (s=1) and for isolated cylinder (s=1).

For the case of two coupled plasma cylinders the structure has two symmetry axes that cause four classes of excited plasmons with different symmetry (Fig. 5): EE (even symmetry with respect to x and y axes), EO (x – even; y - odd), OE (x – odd; y - even), OO (x – odd; y - odd). Consequently the plasmonic modes of the coupled plasma cylinders can be viewed as bonding and antibonding combinations of plasmons of isolated cylinder.

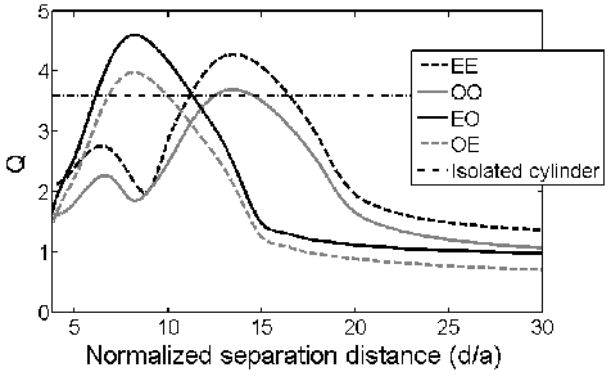

Figure 7. Q-factor for two coupled plasma cylinders (s=1, w_p=1) for EE, OE, EO, OO plasmons and for isolated cylinder (s=1).

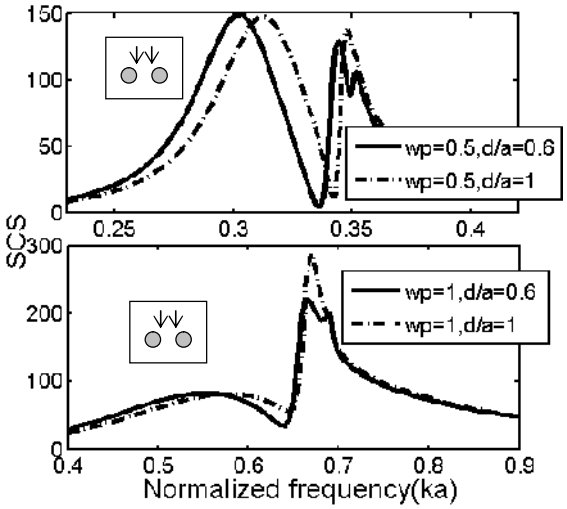

Fig. 8. Scattering cross section of a pair of coupled plasma cylinders versus normalized frequency (ka) for different values of the normalized plasma frequency w_p and for different values of the normalized separation distance. Illumination is along the normal to the main axis.

Figure 6 demonstrates the real values of the eigenfrequencies of the EE, EO, OE, OO plasmons (s=1) for two coupled plasma cylinders ($w_p = 1$) and for isolated cylinder (s=1). It is clearly seen that for distant cylinders eigenfrequencies are nearly identical for all four symmetry classes. As separation distance d becomes smaller, the frequency shift of the coupled plasmons becomes much stronger. The near-field distributions of different plasmons (s=1) of two plasma cylinders are shown in the inset in Fig. 6.

The Q-factor of dipole plasmons in two coupled plasma cylinders (s=1) is shown in Fig. 7. For distant plasma cylinders Q of coupled plasmonic modes is evidently smaller than Q factor of corresponding plasmons of the isolated cylinder. Peaks of Q are observable for the case when separation distance tends to the wavelength.

Figure 8 shows the spectral response of a pair of coupled plasma cylinders for different separation distances between them and different values of the normalized plasma frequency w_p. Direction of illumination is shown in the inset. Upper panel shows Scattering Cross Section of two coupled cylinders with $w_p = 0.5$. First peak corresponds to the excited dipole plasmon ($s = 1$) for both lines. Second one corresponds to the excited quadrupole plasmon ($s = 2$) for distant cylinders ($d/a = 1$), when cylinders are placed closer we see an additional peak associated with $s = 3$ plasmon. Similar phenomenon is shown in the low panel for $w_p = 1$ that can be viewed as cylinder of greater radius. Here dipole plasmon is characterized by first broad low peak. Maximum is associated with quadrupole plasmon for distant cylinders ($d/a = 1$), splitting of the resonance is seen for closely located cylinders ($d/a = 0.6$).

In a linear chain of coupled cylinders bonding and antibonding modes appear in each symmetry class. We have to mention the total number of excided plasmons for each value of s twice greater that number of cylinders in a chain.

Figure 9 shows the Q factor of a variety of EE plasmons. We see the growing of Q with increasing the number of cylinders in a chain, besides the Q for antibonding plasmons exceed those for bonding ones.

For the case of cluster of square configuration shown in Fig. 2 the structure has four symmetry axes associated with horizontal, vertical, and oblique axes that causes six classes of excited plasmons with different symmetry: EEEE, EOEO, OEOE, OOOO, EEEO, OOOE (see Fig. 10). Figure 11 shows the real values of the eigenfrequencies of the EEEE, EOEO, OEOE, OOOO, EEEO and OOOE plasmons (s=2) for cluster of four coupled plasma cylinders ($w_p = 1$) and for isolated cylinder (s=2).

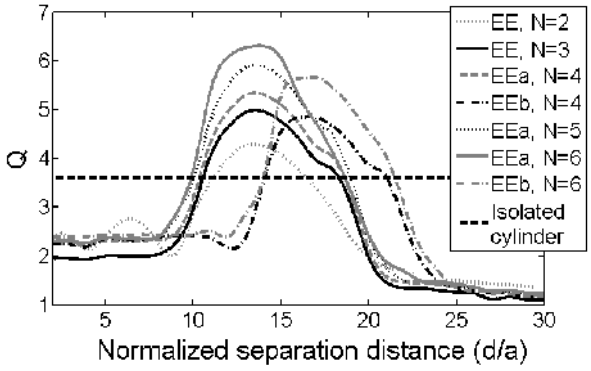

Figure 9. Q-factor for chain of N coupled plasma cylinders (s=1, w_p=1) for EE plasmons and for isolated cylinder (s=1).

With the decreasing of the separation distance between the plasma cylinders we see decreasing of the resonant frequency for EEEE, OEOE, EEEO and OOOE plasmons and increasing for the OOOO and EOEO plasmons.

The Q-factor of plasmons of cluster of four coupled plasma cylinders (s=2) is shown in Fig. 12. We examined the

range of normalized separation distance from 0 to 53. Peaks of Q are observable for separation distance equal the nearly 4-5 wavelength. Maximum peak of Q-factor is seen for OOOE plasmon. Figure 13 demonstrates the near-field portraits of different plasmons of cluster of four coupled plasma cylinders for *s=2* for *d/a*=0.5.

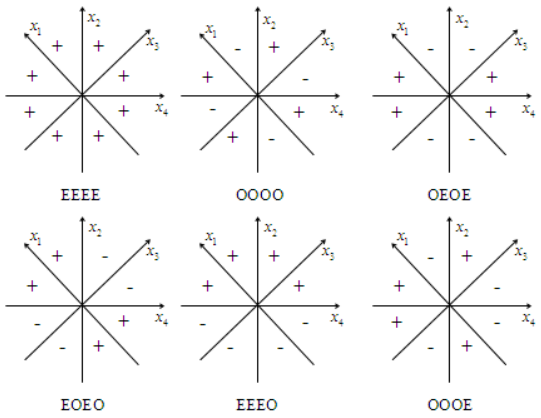

Fig. 10.Six classes of symmetry of the field for the cluster for four coupled cylinders.

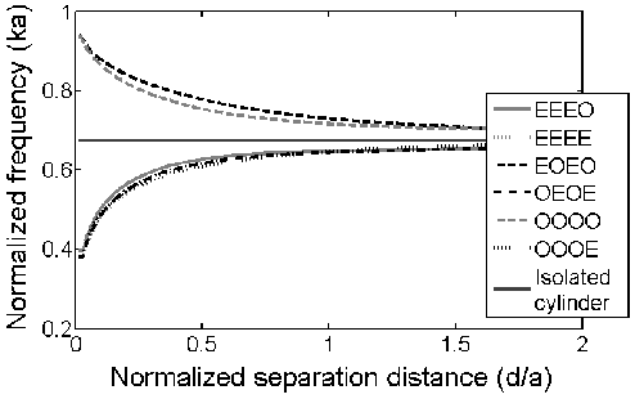

Figure 11. The normalized frequency versus the normalized separation distance between the coupled plasma cylinders in a cluster for different plasmons (*s*=2) and for isolated cylinder.

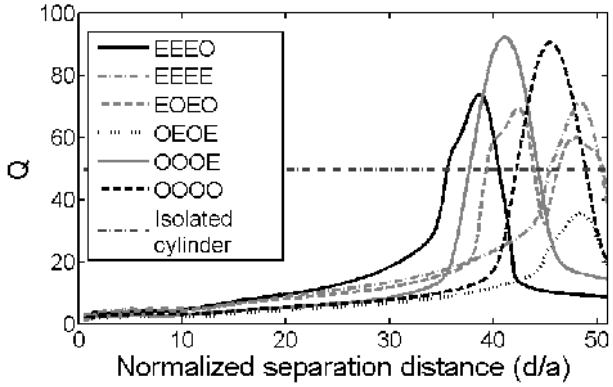

Figure 12. Q-factor for cluster of four coupled plasma cylinders (*s=2*, w_p=1) and for isolated cylinder (*s*=2).

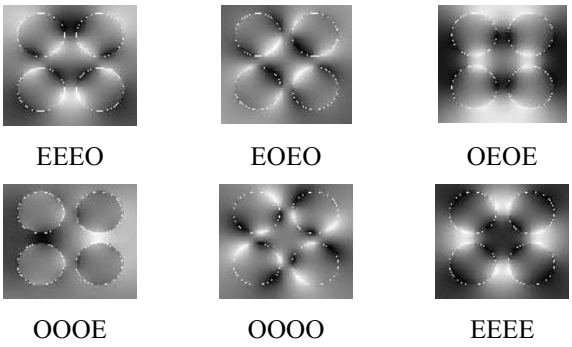

Figure 13. The near-field distributions of plasmons of cluster of four coupled plasma cylinders for *s*=2 *(d/a*=0.5*)*.

IV. CONCLUSIONS

The eigenfrequencies of the coupled cylindrical columns filled with negative permittivity plasma have been analyzed. It has been shown that individual plasmons of isolated column interact and form bonding and antibonding plasmonic coupled modes of different types. Accurate analysis of the influence of the coupling of plasma cylinders on their spectrum of different plasmon resonances is presented. Frequency characteristics of coupled cylindrical plasma aggregates are studied.

ACKNOWLEDGMENT

Ms. N. Stognii wishes to acknowledge to the German Academic Exchange Service (DAAD). Dr. N. Sakhnenko is thankful to the European Science Foundation Research Networking Programme PLASMON-BIONANOSENSE.

REFERENCES

[1] J. Kottmann and O. Martin, "Plasmon resonant coupling in metallic nanowires," Optics Express, vol. 8, 2001, pp. 655-663.

[2] N. Sakhnenko, N. Stognii, A. Nerukh, "Hybridization of Plasmons in Coupled Nanowires," Int. Conf. on Micro- and Nano-photonics material and devices (MINAP-2012), Trento, Italy, 2012, pp. 69-72.

[3] H. R. Stuart, A. Pidwerbetsky, "Electrically small antenna elements using negative permittivity resonators," IEEE Trans. Antennas and Propagation, vol. 54, 2006, pp. 1644-1653.

[4] Y. Zhao, Y. Hao, "Finite-difference time-domain study of guided modes in nano-plasmonic waveguides," IEEE Trans. Antennas Propag., vol. 55. pp. 3070-3077, November 2007.

[5] J. Li, N. Engheta, "Ultracompact sub-wavelength plasmonic cavity resonator on a nanowire," Phys. Rev. B, vol. 74, 2006, pp. 115125.

[6] P. Muhlschlegel, H. Eisler, O. Martin, B. Hecht, D. Pohl, "Resonant optical antennas," Science, vol. 308, 2005, pp. 1607 - 1609.

[7] M. Noginov, G. Zhu, A. Belgrave, R. Bakker, V. Shalaev, E. Narimanov, S. Stout, E. Herz, T. Suteewong, and Wiesner, "Demonstration of a spaser-based nanolaser," Nature, vol. 460, 2009, pp. 1110-1113.

[8] K. Kim, S.J. Yoon, D. Kim, "Nanowire-based enhancement of localized surface plasmon resonance for highly sensitive detection: a theoretical study," Optics Express, vol. 14, №25, 2006, pp. 12419-12431.